1.E.1:
2.G

Nuclear Physics **A346** (1980) 303–323; © *North-Holland Publishing Co., Amsterdam*

SINGLE-PARTICLE AND CORE-EXCITED STATES IN ^{49}Sc (II). The ^{48}Ca(α, t)^{49}Sc reaction

S. FORTIER, I. FODOR-LOVAS †, E. HOURANI ††, J. M. MAISON and J. P. SCHAPIRA

Institut de Physique Nucléaire, BP No. 1, 91400 Orsay, France

Received 22 May 1980

Abstract: The ^{48}Ca(α, t)^{49}Sc reaction has been studied at 36 MeV incident energy. About eighty levels have been observed up to 7.5 MeV excitation energy and angular distributions were measured from 6° to 58°, using a split-pole spectrometer. A local zero-range DWBA analysis has been carried out, and the deduced l-assignments and spectroscopic factors are compared with those obtained from the (^{3}He, d) reaction. In the other hand, a large number of angular distributions cannot be reproduced by the DWBA calculations; they have been compared with the results of coupled-reaction-channel calculations, assuming two-step excitation of weak coupling states with a [^{48}Ca* $\otimes$ $f_{7/2}$] structure. Good agreement between experimental angular distributions and two-step predictions is obtained for several ^{49}Sc levels, suggesting spin and parity assignments. Moreover, as rather large cross sections are predicted for two-step excitations, it is concluded that, generally, these processes cannot be neglected in the analysis of (α, t) reactions.

E | NUCLEAR REACTIONS ^{48}Ca(α, t), E = 36 MeV; measured $\sigma(E_\alpha, \theta)$. ^{49}Sc deduced levels, l, S. DWBA and CRC analyses. Enriched target.

1. Introduction

A large amount of information about nuclear levels has been obtained from the study of one-nucleon-transfer reactions, with a distorted-wave Born approximation (DWBA) analysis assuming a direct one-step transfer of the nucleon. However, for some transitions, the direct mechanism may be in fact forbidden because of the structure of the final states, and higher-order mechanisms such as two-step processes may predominate. This should in particular be the case for core-excited states, due to the coupling of one nucleon (or one hole) with the low-lying excited states of the target nucleus, especially when a high spin value prevents any configuration mixing with single-particle states.

As a matter of fact, a recent study of the (^{3}He, α) reaction on several f-p shell nuclei [1,2]) has shown that original information about core-excited states can be

† Visitor from the Institute for Physics of the Hungarian Academy of Sciences, Budapest, Hungary.
†† Permanent address: Lebanese University, Faculty of Sciences, Hadat-Beyrouth, Lebanon.

obtained from one-nucleon transfer reactions, by a detailed investigation of weak transitions and a subsequent coupled-reaction-channel (CRC) analysis, taking two-step mechanisms into account. It has been particularly pointed out that two-step angular distributions strongly depend on the spin value of the final state, thus suggesting a new method for spin assignments. For example, angular distributions measured in the ^{48}Ca(^{3}He, α)^{47}Ca reaction [1]) have allowed one to identify some ^{47}Ca levels with core-excited states, due to the coupling of one $f_{\frac{7}{2}}$ neutron hole with low-lying excited states in ^{48}Ca, and subsequent spin assignments have been proposed.

In a similar way, it should be possible to identify core-excited states in ^{49}Sc – with one $f_{\frac{7}{2}}$ proton coupled to the ^{48}Ca core – through a CRC analysis of a proton stripping reaction, provided that the cross sections for two-step excitations are not too low, and that the corresponding angular distributions have a characteristic pattern. In the preceding paper (I), we have presented a study of the ^{48}Ca(^{3}He, d)^{49}Sc reaction at 25 MeV; it was shown that most results can be easily interpreted in the framework of a conventional DWBA analysis, giving a great deal of information about the fragmentation of single-particle states in ^{49}Sc. The investigation of the ^{48}Ca(α, t)^{49}Sc reaction at 36 MeV reported here was mainly undertaken to study the influence of two-step effects and eventually identify core-excited states in ^{49}Sc.

The application of the (α, t) reaction to spectroscopy has been up to now mostly limited to the study of levels excited with a large value of transferred angular momentum ($l \geqq 4$), thus complementing the results obtained for lower l-transfers from other proton stripping reactions [3]). In fact, due to the angular momentum mismatch between the entrance and exit channels, the (α, t) reaction is known to preferentially transfer a large amount of angular momentum, and the DWBA analysis is generally not straightforward for low l-transfers, as shown in refs. [4-7]). It was suggested [4]) that two-step processes could play an important part in the reaction mechanism, and thus be partly responsible for the difficulties encountered in the DWBA analysis. The results of a standard DWBA analysis of the ^{48}Ca(α, t)^{49}Sc reaction are presented in sect. 3, and compared with those obtained in a previous study [7]) of the same reaction, and with the (^{3}He, d) results of paper I. On the other hand, the cross sections expected for two-step processes in the (α, t) reaction have been calculated with the CRC method. They are reported in sect. 4, and compared with the experimental data. It will be shown that two-step effects cannot anyway be neglected in the analysis of (α, t) reactions. The spectroscopic results deduced for ^{49}Sc are summarized in sect. 5, and spin and parity assignments are suggested for a number of low-lying levels, based on the comparison of angular distributions with CRC predictions.

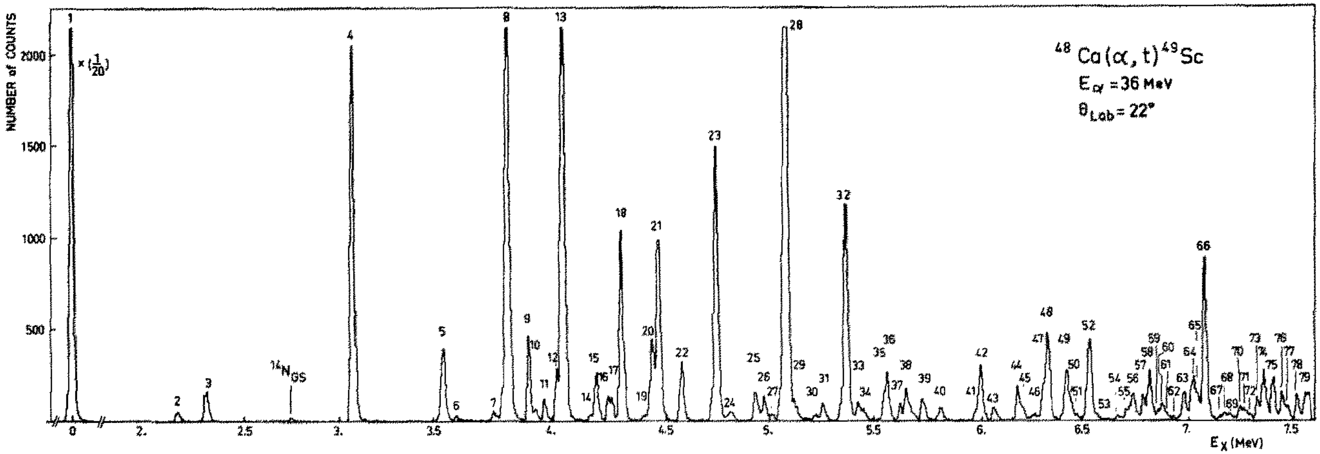

Fig. 1. Triton spectrum from the $^{48}Ca(\alpha, t)^{49}Sc$ reaction at 22° (lab), observed in the focal plane of the split-pole spectrometer. The numbers on the top of the peaks refer to the ^{49}Sc levels reported in table 1.

TABLE 1

Results of the DWBA analysis of the ^{48}Ca(α, t)^{49}Sc reaction at 36 MeV, and comparison with previous (α, t) and (^{3}He, d) data

		^{48}Ca(α, t)^{49}Sc E_α = 36 MeV (present work)			^{48}Ca(α, t)^{49}Sc E_α = 44 MeV [ref. [7]]			^{48}Ca(^{3}He, d)^{49}Sc $E_{^3He}$ = 25 MeV (paper I)		
Peak no.	E_x [a]) (MeV)	$(d\sigma/d\Omega)_{c.m.}$ at 6° lab (mb/sr)	l	$(2J+1)C^2S$ [b])	E_x (MeV)	l	$(2J+1)C^2S$	E_x (MeV)	l	$(2J+1)C^2S$
1	0	40.8	3	6.72	0	3	8.0	0	3	6.72
2	2.229	0.15	0	0.14	2.21	0	0.09	2.229	0	0.03
3	2.372	0.16	2	0.16	2.38	2	0.10	2.372	2	0.05
4	3.084	4.2	1	1.24	3.08	1	1.35	3.084	1	2.08
5	3.514	0.14			3.52	1	0.28	3.517		
6	3.581	0.010								
7	3.750	0.030	2	0.04				3.755	2	0.01
8	3.808	2.38	(3)	0.60	3.81	3	1.31	3.809	3	0.53
9	3.916	0.046						3.921		
10	3.951	0.006								
11	3.992	0.16	0	0.21				3.992	0	0.02
12	4.041	0.040								
13	4.069	2.18	3	1.02	4.08	3	1.31	4.072	3	0.98
14	4.192	0.005								
15	4.218	0.020						4.220		
16	4.267	0.028								
17	4.286	0.066						4.285		
18	4.326	0.88	3	0.41	4.34	3	0.61	4.333	3	0.44
19	4.426	0.015								
20	4.459	0.36								
21	4.488	0.97	1	0.67	4.49	1	(0.54)	4.495	1	1.04
22	4.580	0.043						4.579	1	0.02
23	4.742	1.42	3	0.78	4.76	3	0.68	4.738	3	0.70
24	4.825	0.032	(2)					4.810	3	0.03
25	4.946	0.025			4.95	1	0.33	4.948	(1)	0.001
26	4.987	0.017								
27	5.022	0.15	0	0.20 [c])				5.015	1	0.19
28	5.086	3.21	3	1.93	5.12	3	1.56	5.077	3	1.99
29	5.142	0.02								
30	5.229	0.021	5	0.006				5.230	2	0.02
31	5.269	0.055								
32	5.373	1.32	3	0.83	5.43	3	0.71	5.380	3	0.81
33	5.431	0.033						5.438		
34	5.460	0.006								
35	5.562	0.096	5	0.21						
36	5.576	0.033						5.578	2	0.05
37	5.632	0.018								
38	5.664	0.22	(1)	0.25	5.71	(1)	0.30	5.663	1	0.39
39	5.735	0.036								
40	5.815	0.098	(1)	0.14				5.815	1	0.08
41	5.979	0.033								
42	6.000	0.23	(2)	0.09				6.000		

TABLE 1 (continued)

		^{48}Ca(α, t)^{49}Sc E_α = 36 MeV (present work)			^{48}Ca(α, t)^{49}Sc E_α = 44 MeV [ref. [7]]			^{48}Ca(^{3}He, d)^{49}Sc $E_{^3\mathrm{He}}$ = 25 MeV (paper I)		
Peak no.	E_x [a]) (MeV)	$(d\sigma/d\Omega)_{c.m.}$ at 6° lab (mb/sr)	l	$(2J+1)C^2S$ [b])	E_x (MeV)	l	$(2J+1)C^2S$	E_x (MeV)	l	$(2J+1)C^2S$
43	6.064	0.018						6.069	(2)	0.02
44	6.189	0.062						6.180	2	0.08
45	6.212	0.031								
46	6.259	0.016						6.250		
47	6.311	0.052						6.307		
48	6.330	0.11								
49	6.422	0.30	3	0.15				6.412	3	0.14
50	6.451	0.035								
51	6.476	0.005								
52	6.534	0.037						6.527	1+4	0.03+0.20
53	6.624	0.004								
54	6.681	0.004						6.685		
55	6.716	0.061	3	0.05				6.717	1	0.06
56	6.745	0.13								
57	6.799	0.058						6.811	1	0.13
58	6.829	0.20	3	0.20						
59	6.867	0.008								
60	6.889	0.078	0	0.08 [c])				6.910	0	0.02
61	6.917	0.018								
62	6.939	0.010								
63	6.981	0.12	(3)	0.13				6.981	3	0.14
64	7.018	0.13						7.026	1	0.04
65	7.041	0.038								
66	7.076	0.56	(4)	0.19				7.059	1+4	0.08+0.41
67	7.149	0.017	3					7.151		
68	7.172	0.007								
69	7.200	0.025	(4)	0.01				7.186		
70	7.244	0.032								
71	7.268	0.020						7.253	1	0.01
72	7.293	0.007								
73	7.326	0.10	3	0.12				7.320	1	0.06
74	7.354	0.18	(3)	0.20				7.342	3	0.22
75	7.396	0.18	(3)	0.20				7.375	3	0.18
76	7.441	0.086	(3)	0.10				7.421	3	0.08
77	7.465	0.026						7.442	1	0.01
78	7.510	0.12	3	0.14				7.483	3	0.14

[a]) The accuracy about excitation energies is estimated better than 10 keV. Excitation energies from the (^{3}He, d) experiment are given with an uncertainty of about 8 keV below 6 MeV and 20 keV above.

[b]) For levels with unknown spin value, the spectroscopic factors were determined using the same spin assumptions as in the analysis of the (^{3}He, d) reaction in paper I: i.e. $\frac{1}{2}^-$ for $l = 1$ transitions except for the level at 3.08 MeV, $\frac{5}{2}^+$ for the $l = 2$ levels above 4 MeV, $\frac{7}{2}^-$ for the $l = 3$ levels above 4 MeV, and $\frac{9}{2}^+$ and $\frac{11}{2}^-$ for the $l = 4$ and 5 levels, respectively.

[c]) Spectroscopic factor determined for a $3s_{1/2}$ transfer.

2. Experimental procedure

The ^{48}Ca(α, t)^{49}Sc reaction was studied at 36 MeV incident energy with the MP tandem accelerator at Orsay. The tritons were detected with six 1000 μm thick position-sensitive Si detectors, placed in the focal plane of a split-pole spectrometer. The calcium target, 97.2 % enriched in ^{48}Ca, was supported on a thin carbon film: its thickness was about 100 μg/cm^2. The uncertainty of the absolute cross sections, deduced from the target thickness and the solid angle of the spectrometer, is estimated to be about 30 %. Angular distributions were measured in 4° steps, from 6° to 58° (lab). Two successive exposures at different magnetic fields were necessary at each angle in order to cover the spacings between adjacent detectors in the focal plane. The triton spectrum presented in fig. 1 was obtained by juxtaposing individual spectra in each detector for both exposures. About 80 levels are observed in the 0 to 7.5 MeV excitation energy range, with an overall energy resolution of about 20 keV.

A calibration of the radius ρ versus the channel number was obtained by observing the positions of the peaks formed in the (α, t) reaction on a natural titanium target, as the Q-values and excitation energies for the different isotopes are well known and tabulated. The subsequent observation of the (α, t) spectrum on ^{48}Ca, at the same value of the magnetic field, led to a determination of excitation energies in ^{49}Sc with an accuracy estimated better than 10 keV. These excitation energies are listed in table 1 and compared with those deduced in paper 1 from the (^{3}He, d) reaction. A number of low-lying levels, previously unknown, are observed in the (α, t) reaction, whereas they could not be detected in (^{3}He, d) because of poorer energy resolution and lower cross sections. The differential cross sections measured at 6° (lab) are indicated in table 1 for all ^{49}Sc levels observed in the (α, t) reaction.

3. Distorted-wave analysis

3.1. DWBA CALCULATIONS

Zero-range DWBA calculations were performed with the code DWUCK [8]). The form factor for the transferred proton was calculated using the standard separation energy procedure, where the depth of the Woods-Saxon well is adjusted in order to reproduce the experimental binding energies. Geometrical parameters of the proton well are given in table 2, with two different sets of optical parameters for both entrance and exit channels. The theoretical angular distributions obtained with the different combinations of α and t optical potentials are compared in fig. 2 with the experimental data for the $f_{\frac{7}{2}}$ ground state and the $p_{\frac{3}{2}}$ state at 3.08 MeV.

It can be noticed that the $l = 1$ angular distribution is more sensitive to the choice of optical potentials than the $l = 3$ one. This could be predicted considering the

TABLE 2

Optical-model potentials [a]) used in the DWBA and CRC calculations

Particle	V_0 (MeV)	r_0 (fm)	a_0 (fm)	W (MeV)	r'_0 (fm)	a'_0 (fm)	r_{0C} (fm)
p	U_0	1.25	0.65				
α { set α_1 [b])	206.3	1.37	0.56	25.1	1.37	0.56	1.4
α { set α_2 [c])	200.2	1.354	0.586	52.04	1.354	0.586	1.4
t { set t_1 [d])	V_t	1.20	0.72	W_t	1.40	0.84	1.3
t { set t_2 [e])	176.0	1.14	0.71	14.68	1.669	0.799	1.4

[a]) The potentials for α-particles and tritons were of the form: $V(r) = V_C - V_0 f(x) - iWf(x')$, where $f(x_i) = (1+e^{x_i})^{-1}$, with $x = (r - r_i A^{1/3})/a_i$ and V_C is the Coulomb potential. The form factors are computed with a binding potential $U(r) = -U_0\,[f(x) - \lambda \boldsymbol{L}\cdot\boldsymbol{S}/45.2\,(\mathrm{d}/\mathrm{d}x)f(x)]$ with $\lambda = 25$.

[b]) Ref. [10]). [c]) Ref. [11]).

[d]) Ref. [12]), $V_t = 165.0 - 0.17E - 6.4(N-Z)/A$, $W_t = 46.0 - 0.33E - 110(N-Z)/A$.

[e]) Ref. [13]).

mismatch between the $l = 1$ transferred angular momentum and the semi-classical momentum $|\boldsymbol{k}_f - \boldsymbol{k}_i|R$, approximately equal to 4: in such a case, it is well known that a significant contribution to the reaction is given by inner partial waves, to which elastic scattering data are insensitive. The sets of optical parameters "$\alpha_1 - t_1$" (cf table 2) was finally adopted in the calculations.

The validity of the zero-range approximation for the (α, t) reaction at 36 MeV was tested in performing finite-range DWBA calculations with the code

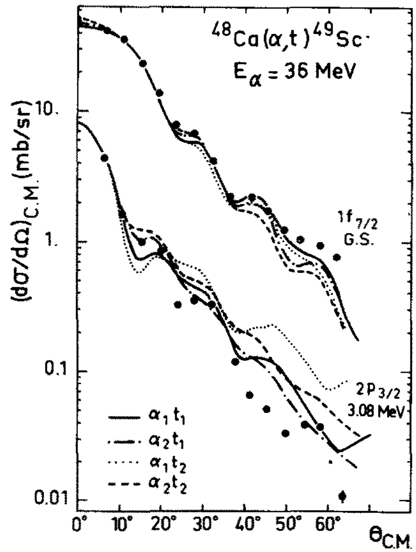

Fig. 2. DWBA predictions, using four different combinations of the optical parameters reported in table 2, for the α-particle and triton channels.

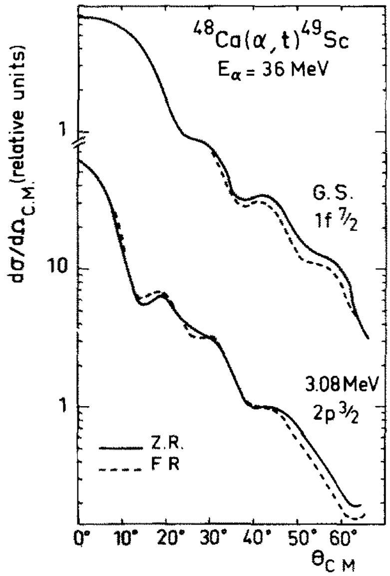

Fig. 3. Comparison of zero-range (ZR) and finite-range (FR) DWBA predictions for the $^{48}Ca(\alpha, t)^{49}Sc$ reaction at 36 MeV.

MARY [14,15]) for $f_{\frac{7}{2}}$ and $p_{\frac{3}{2}}$ transfers. The finite-range results are compared in fig. 3 with those obtained from the code DWUCK. As the shapes of the angular distributions are very similar, finite-range effects can be reasonably considered as negligible.

Some examples of theoretical shapes of angular distributions predicted for various values of the transferred angular momentum are displayed in figs. 4–7 and compared with the experimental data. In the cases where an l-assignment was possible, spectroscopic factors C^2S were deduced from the theoretical cross sections, $\sigma_{\mathrm{DW}}^{lj}$, by means of the expression,

$$(\mathrm{d}\sigma/\mathrm{d}\Omega)_{\mathrm{exp}} = NC^2S\sigma_{\mathrm{DW}}^{lj}. \tag{1}$$

The normalization factor N for the (α, t) reaction is here taken equal to 40, in rather good agreement with previous determinations. With this normalization factor, the spectroscopic factor determined for the $f_{\frac{7}{2}}$ ground state is found equal to the value obtained from the (^{3}He, d) analysis of paper I.

3.2. RESULTS

The results of the DWBA analysis are summarized in table 1. Assignments of l-values are proposed for about thirty levels in ^{49}Sc. The results obtained in a previous study of the ^{48}Ca(α, t)^{49}Sc reaction, together with the (^{3}He, d) results of paper I, are also given for comparison.

$l = 3$ transitions: Up to 6.5 MeV excitation energy, almost all the $l = 3$ transitions observed in (^{3}He, d) are also seen in (α, t) with angular distributions rather well reproduced by DWBA (cf. fig. 4). Moreover, with the (α, t) normalization factor adopted in the present analysis the spectroscopic factor deduced from these two

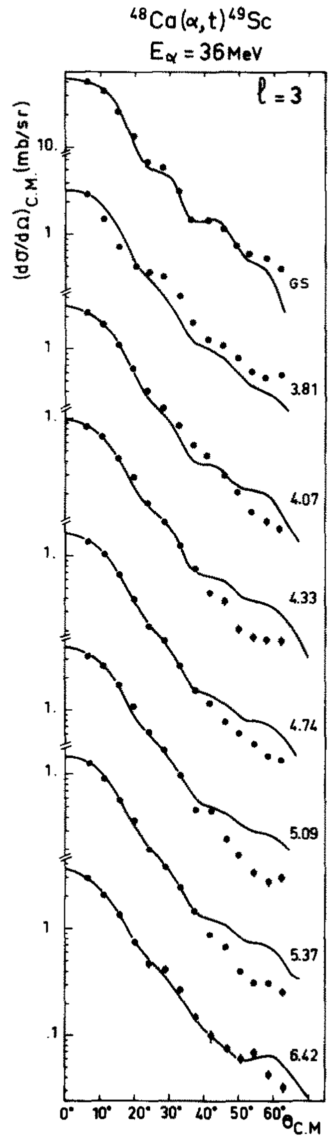

Fig. 4. Experimental angular distributions compared to DWBA predictions for $l = 3$ transfers.

reactions are in excellent agreement, thus supporting the DWBA assumption of a pure direct $l = 3$ proton transfer to the final levels. A noticeable exception is however observed in fig. 4 for the 3.81 MeV level, with previously determined [16]) spin and parity $\frac{7}{2}^-$, which displays an angular distribution different from that expected for a pure $l = 3$ transfer. The eventuality for a competing two-step process for exciting this level will be discussed in sect. 4.

l = 1 transitions: In spite of the large angular momentum mismatch existing for low l-transitions in (α, t), angular distributions are correctly reproduced by DWBA for the strong $l = 1$ transitions at 3.08 and 4.49 MeV, respectively identified [17]) with the main component of the $p_{\frac{3}{2}}$ and $p_{\frac{1}{2}}$ single-particle states (cf. fig. 5). However, the spectroscopic factors extracted from (α, t) are about 40 % lower than those from the (^{3}He, d) reaction. Many weaker $l = 1$ transitions have also been observed in the (^{3}He, d) reaction, but the (α, t) angular distributions observed for the same final levels in ^{49}Sc do not generally display an $l = 1$ character. Finally, the $l = 1$ assignment proposed in ref. [17]) for the levels at 3.52 and 4.95 MeV are not confirmed in the present analysis of (^{3}He, d) and (α, t) reactions.

l = 2 transitions: The angular distributions observed for the levels at 2.37 and 3.75 MeV are fitted by DWBA, assuming a proton transfer in the $1d_{\frac{3}{2}}$ inner subshell. This l-assignment is in good agreement with the (^{3}He, d) results, but a discrepancy between the spectroscopic factors deduced from the two reactions is however observed.

l = 0 transitions: It has been emphasized in subsect. 3.1 that, in the case of transitions with angular momentum mismatch, the DWBA predictions are very sensitive to the contributions of the inner part of the nucleus. This fact is illustrated in figs. 5 and 6 for $l = 0$ angular distributions, displaying a strong dependence on the number of nodes in the wave function of the transferred proton. The experimental (α, t) angular distributions suggest that the transitions to the levels at 2.23 MeV and 3.99 MeV proceed through a transfer in the $2s_{\frac{1}{2}}$ inner shell, whereas a transfer in the $3s_{\frac{1}{2}}$ orbital is involved for the higher-lying levels at 5.02 and 6.89 MeV. The $l = 0$ assignment is in agreement with (^{3}He, d) results, except for the 5.02 MeV level: in the same energy region, a $l = 1$ transition is in fact observed in the (^{3}He, d) reaction. One explanation for this conflicting assignment could be the existence of two distinct closely spaced levels, each of them being preferentially excited in one of the two reactions. A discussion about the structure of the 5.02 MeV level observed in the present reaction will be done in sect. 4.

l = 4 and l = 5 transitions: Theoretical angular distribution for $l = 4$ and $l = 5$ transfers are structureless, and they are only slightly different from those predicted for $l = 3$. So it is generally difficult to propose an unambiguous l-assignment with $l \geqq 3$, based only on the results of the (α, t) reaction. A tentative $l = 4$ assignment is done for the level at 7.08 MeV, which would then correspond to the strongest $l = 4$ transition observed in the (^{3}He, d) reaction (cf. fig. 5). Deduced from the angular distributions displayed in fig. 6, a $l = 5$ assignment is proposed for the levels

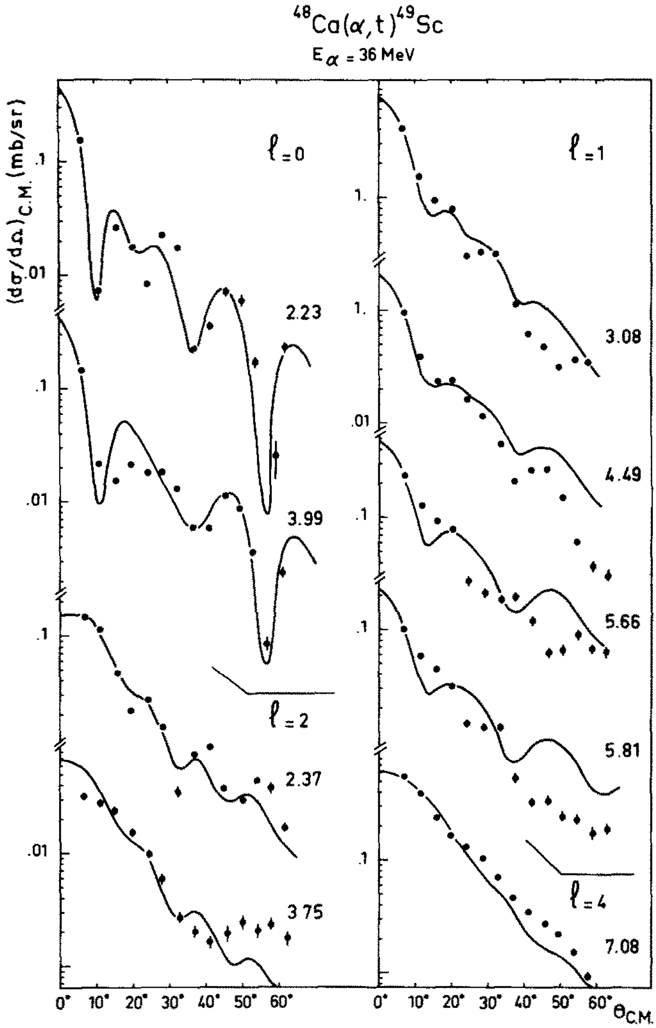

Fig. 5. Examples of angular distributions compared to DWBA predictions for l = 0, 1, 2 and 4 transfers (the calculations for l = 0 and l = 2 are done assuming a proton stripping to the inner $2s_{1/2}$ and $1d_{3/2}$ subshells, respectively).

at 5.23 and 5.56 MeV, which could be low-lying weak components of the $1h_{\frac{11}{2}}$ strength in ^{49}Sc.

Other transitions: A large number of previously unknown ^{49}Sc levels are observed in the present experiment, with differential cross sections lower than 100 μb/sr. For most of these weak (α, t) transitions, the experimental angular distributions are completely different from those calculated in the DWBA frame. These angular distributions are shown in fig. 7. One has to emphasize that these "non-stripping"

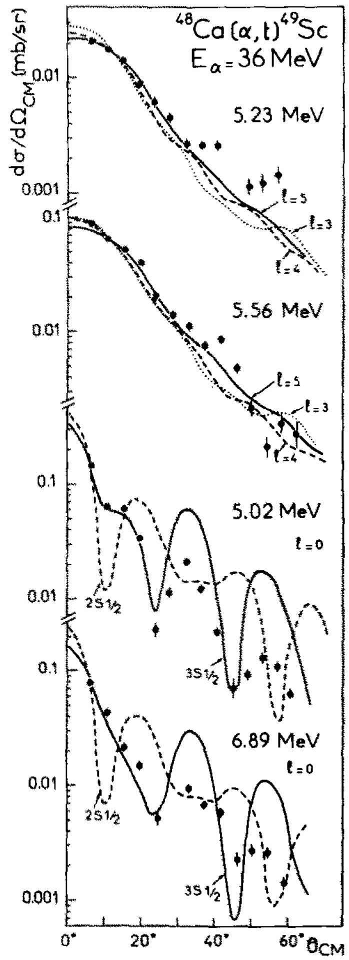

Fig. 6. Comparison of experimental angular distributions with the DWBA predictions for a stripping to $1h_{11/2}$ and $3s_{1/2}$ orbitals. A comparison is also done with the predictions for other transfers; in particular the difference between the angular distributions for a $2s_{1/2}$ and $3s_{1/2}$ transfer is clearly observed.

angular distributions are not at all structureless, but generally display more or less oscillatory patterns. The possibility that these angular distributions could characterize a two-step excitation of core-excited states is now examined.

4. Coupled-reaction-channel analysis

Differential cross sections for two-step excitations can be calculated with the CRC method. However, as the reaction can generally proceed through several

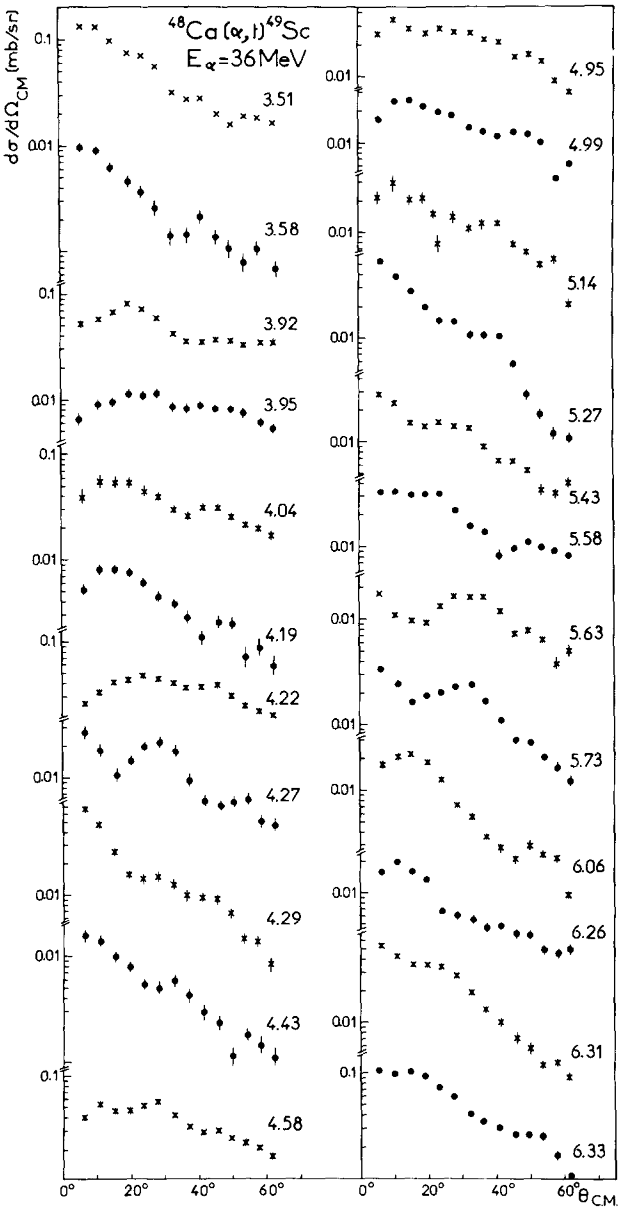

Fig. 7. Angular distributions with a non-stripping character observed in the $^{48}Ca(\alpha, t)^{49}Sc$ reaction.

paths, it is necessary to specify the wave functions of the nuclear states involved in the reaction mechanism, in order to calculate the interference effects. The present CRC calculations have been performed using the simplifying assumption of the weak-coupling model. The predictions of the weak-coupling model are shown in

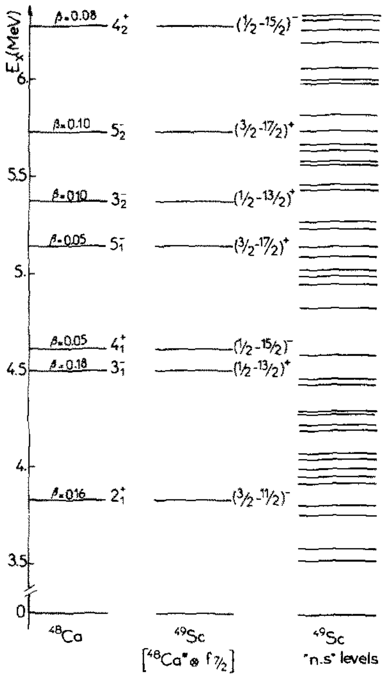

Fig. 8. Energies of "non-stripping" (n.s.) levels in ^{49}Sc, compared with those predicted for weak-coupling multiplets. The corresponding low-lying states in ^{48}Ca are also indicated, with their β-values deduced from inelastic excitation experiments.

fig. 8. The "non-stripping" levels under study are in fact observed in the energy region predicted for weak-coupling multiplets $[\lambda \otimes f_{\frac{7}{2}}]$ resulting from the coupling of one $f_{\frac{7}{2}}$ proton to the low-lying ^{48}Ca states with spin λ, and it is hoped that the weak-coupling model could be a good approximation for the structure of some of these levels. The excitation of pure weak coupling states through a direct proton transfer is forbidden, due to the lack of a single-particle component in the final wave functions, and the natural way of exciting them should then be a two-step process, with the $f_{\frac{7}{2}}$ transfer coupled to an inelastic excitation. There are in fact two possible paths, here denoted (α, α', t) and (α, t, t'), according to whether the inelastic excitation takes place in the entrance or the exit channel, and the interference between these two processes has to be taken into account in the calculations.

4.1. DIFFERENTIAL CROSS SECTIONS FOR PURE WEAK-COUPLING STATES

The CRC code CHUCK2 [ref. [18])] was used to calculate the angular distributions expected for the different weak coupling states shown in fig. 8. Optical potentials for the α- and t-channels were those used in the DWBA analysis (see table 2). Inelastic excitations in ^{48}Ca and ^{49}Sc were assumed to proceed one-way directly

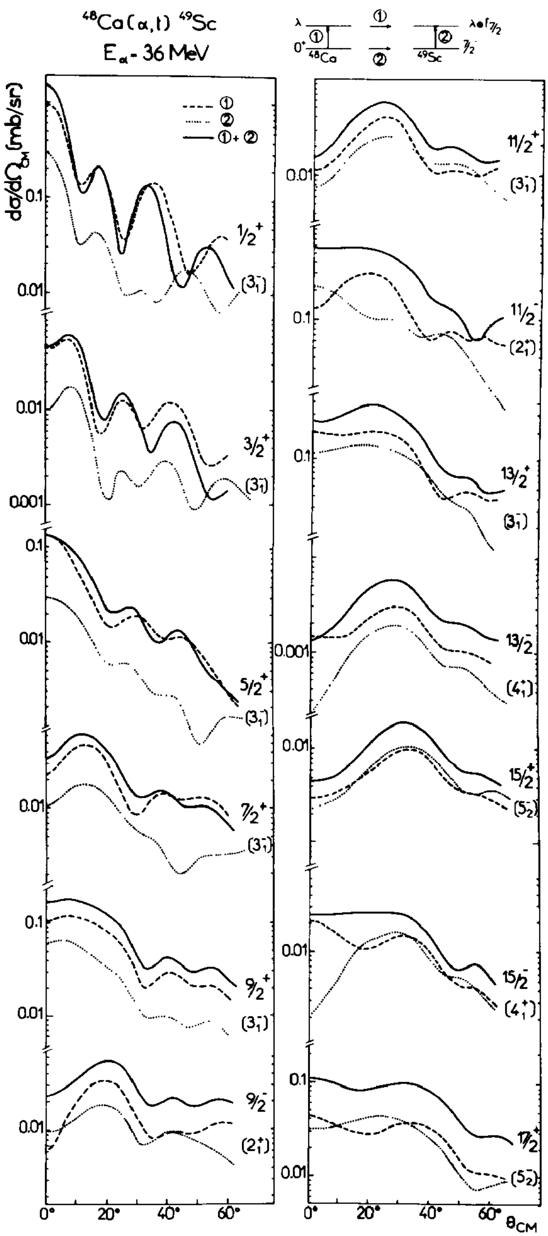

Fig. 9. Examples of CRC predictions for two-step excitation of weak coupling states (the corresponding low-lying ^{48}Ca state λ is specified within parantheses for each angular distribution). The differential cross-sections for the (α, α', t) and (α, t, t') processes alone are indicated with dashed and dotted lines, respectively, whereas the results of the interference calculations are given with the full lines.

from the ground state. The deformation parameters β, used for the ^{48}Ca excited states and the corresponding multiplets in ^{49}Sc, were extracted from an analysis [19]) of the ^{48}Ca (p, p')^{48}Ca reaction; they are reported in fig. 8. According to the weak-coupling assumption, the coupling strength for the ($\lambda \rightarrow J$) $f_{\frac{7}{2}}$ transition was taken equal to that used for the transition between the ^{48}Ca and ^{49}Sc ground states, multiplied by the phase factor $(-)^{\lambda+J+3j}$ (where j is the transferred angular momentum, equal to $\frac{7}{2}$ in the present case). In the present calculation, $\sqrt{C^2S}$ was taken equal to the shell-model sum-rule limit of 1, which is close to the experimental value for the $f_{\frac{7}{2}}$ ground-state transition.

Differential cross sections were calculated separately for the (α, α', t) and (α, t, t') processes, in order to display their individual contribution to the total cross section. Some examples of theoretical angular distribution are shown in fig. 9 for different values of spin and parity (the $\frac{1}{2}^-$ to $\frac{7}{2}^-$ angular distributions are not shown here, as there is a particularly large probability for a configuration mixing with the neighbouring f-p single-particle states). The inelastic excitation in the entrance channel – the (α, α', t) path – appears as the dominant two-step process in most cases; however, the (α, t, t') process contributes to the total cross section in a significant way, especially for high-spin states, and therefore, it should not be neglected in the calculations.

The cross sections for two-step excitations are proportional to β^2, and in fact, the cross sections calculated for the members of the weak-coupling multiplet associated to the first 2^+ and 3^- states in ^{48}Ca, are found to be larger than for the other multiplets. In the other hand, it may be of interest to notice that, for the members of a same multiplet, there is an alternation of small and large cross sections with increasing spin values. This alternation of cross sections, varying by about one order of magnitude, can be observed in fig. 9 for the $[3_1^- \otimes f_{\frac{7}{2}}]$ multiplet, with spin ranging from $\frac{1}{2}$ to $\frac{13}{2}$.

The main feature of the angular distributions in fig. 9 is the dependance on the spin and parity value of the final state, particularly characterized by the increase of the width of the first bump with the spin value. The calculations for the other weak coupling states also show this characteristic J^π dependance, as the differences of angular distributions for levels with the same J^π value, corresponding to different multiplets, are generally small. This spin and parity dependance of (α, t) angular distributions for the two-step excitation of weak coupling states, is quite similar to that observed in the two-step (^{3}He, α) reaction [1,2]).

4.2. COMPARISON WITH THE DATA

The results of the present calculation, performed with the crude assumption of the weak-coupling model, have now to be compared with the experimental data. First, it is observed that the cross sections for "non-stripping" levels are generally around 10 to 100 μb/sr, which is typically the range of cross sections predicted for two-step processes. Moreover, the smooth oscillations experimentally observed

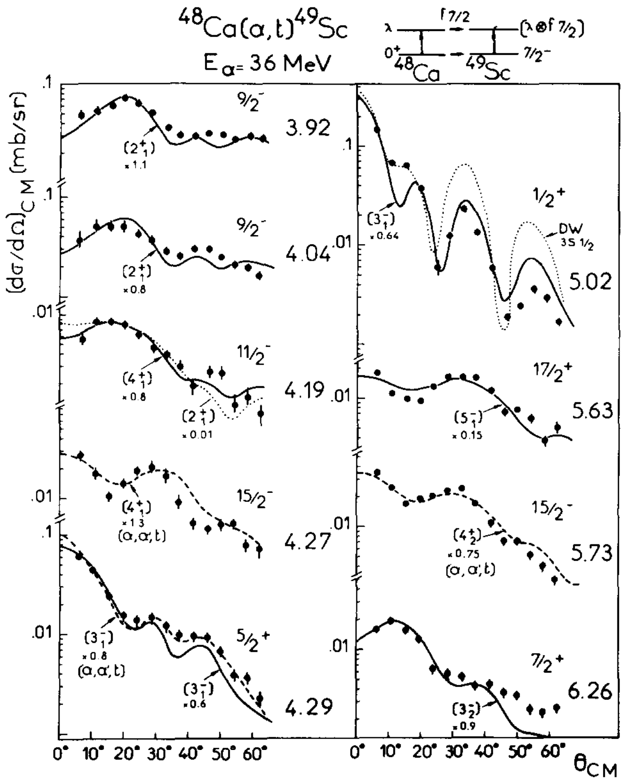

Fig. 10. Comparison of some experimental angular distributions with CRC predictions for two-step excitation of weak-coupling states (see text).

(cf. fig. 7) and those found in the CRC calculations, display a striking analogy for a number of levels. Such a comparison between experimental and theoretical angular distributions is shown in fig. 10 for nine ^{49}Sc levels, illustrating the possible spectroscopic application of the present analysis.

The weak-coupling assumption may be considered as a good approximation for a particular ^{49}Sc level if the experimental and theoretical angular distributions agree in both shape and magnitude: the theoretical cross sections in fig. 10 were multiplied by a normalization factor in order to fit the data; this factor was found reasonably close from the theoretical value of 1, for most of these nine levels. On the other hand, any departure of a pure weak-coupling configuration could in principle alter the shape of the angular distribution, due to additional possible reaction paths and also bring about a change in the relative weights of the (α, α', t) and (α, t, t$'$) contributions. For three of these levels, a better fit is in fact obtained when comparing with the predictions for a pure (α, α', t) process. It is therefore obvious that the J^{π} assignments suggested by the comparisons in fig. 10 and proposed below have to be considered as only tentative and should anyway be confirmed by additional experiments.

The 3.92 MeV level: A $\frac{9}{2}^-$ assignment is proposed for this level. The normalization factor of 1.1 strongly supports its identification with the $\frac{9}{2}^-$ member of the $[2_1^+ \otimes f_{\frac{7}{2}}]$ multiplet, predicted to lie at about 3.75 MeV by the weak-coupling model.

The 4.04 MeV level: A $\frac{9}{2}^-$ angular distribution approximately reproduces the data; however, any conclusion about the structure of this level seems more dubious than in the previous case, due to the relatively large error bars for the date at forward angles.

The 4.19 MeV level: An $\frac{11}{2}^-$ angular distribution is observed for this level, with a cross section close to that calculated for a pure $[4_1^+ \otimes f_{\frac{7}{2}}]$ configuration.

The 4.27 MeV level: The oscillatory pattern observed in its angular distribution is rather similar to that predicted for the $\frac{15}{2}^-$ member of the $[4_1^+ \otimes f_{\frac{7}{2}}]$ multiplet, in the case of a pure (α, α', t) excitation. A $\frac{15}{2}^-$ assignment is therefore tentatively proposed for this level.

The 4.29 MeV level: This level can be tentatively identified with the $\frac{5}{2}^+$ member of the $[3_1^- \otimes f_{\frac{7}{2}}]$ multiplet, predicted to lie at about 4.5 MeV. It can be noticed that, for this level also, a pure (α, α', t) excitation better reproduces the data.

The 5.02 MeV level: The DWBA analysis has suggested that this level was excited through a $l = 0$ direct process, with a transfer of one proton in the $3s_{\frac{1}{2}}$ orbital. Another interpretation of the experimental data can be however proposed, based on the comparison of fig. 10. The angular distribution is in fact well reproduced by the calculations for the two-step excitation of a $\frac{1}{2}^+$ state, with a $[3_1^- \otimes f_{\frac{7}{2}}]$ structure. It is likely that, in actual fact, both direct and two-step processes interfere for exciting this $\frac{1}{2}^+$ level.

The 5.63 MeV level: A $\frac{17}{2}^+$ assignment is proposed for this level. The existence of two $\frac{17}{2}^+$ states in this energy region is in fact predicted by the weak coupling model, as resulting from the coupling of one $f_{\frac{7}{2}}$ proton with the 5^- states at 5.15 and 5.73 MeV.

The 5.73 MeV level: A $\frac{15}{2}^-$ assignment is proposed for this level, as its angular distribution is nicely reproduced by the CRC calculations for an excitation through the (α, α', t) process. This level would then result from the coupling of one $f_{\frac{7}{2}}$ proton with the second 4^+ state at 6.34 MeV.

The 6.26 MeV level: A $\frac{7}{2}^+$ assignment is proposed for this level, which would result from the coupling of one $f_{\frac{7}{2}}$ proton with the 3^- or 5^- states observed below 6 MeV in ^{48}Ca. The experimental cross section suggests a $[3_2^- \otimes f_{\frac{7}{2}}]$ configuration for this level.

4.3. DISCUSSION

The purpose of the present study may be thus considered as partly achieved, as some of the non-stripping angular distributions can be interpreted as resulting from pure two-step excitations, and suggest the identification of the corresponding levels with core-excited states with a definite spin and parity. However, the weak-coupling model used in the CRC analysis because of its simplicity, is clearly unable to reproduce the whole experimental angular distributions of fig. 7. More sophisticated models, involving configuration mixings, would be in fact necessary for describing the structure of core-excited states in ^{49}Sc, and the CRC calculations should then take the interferences between all the possible reactions paths into account.

Interference effects between one-step and two-step transitions are expected, for example, for the levels at 3.52 and 3.81 MeV, with respective J^π values of $\frac{3}{2}^-$ [ref. [17]] and $\frac{7}{2}^-$ [ref. [16]]. These levels lie at an energy close to that predicted for the $[2_1^+ \otimes f_{\frac{7}{2}}]$ multiplet and it is seen in fig. 11 that the theoretical cross sections for the corresponding pure two-step transitions are in fact not at all negligible, compared with the experimental ones. As a small configuration mixing with, respectively, the $p_{\frac{3}{2}}$ and $f_{\frac{7}{2}}$ single-particle states is highly probable, the observed angular distributions are expected to result from an interference between one- and two-step processes. It has been attempted to reproduce the data with a calculation of interference effects, involving various possible ratios of one- and two-step reaction amplitudes. However a substantially better agreement between theoretical and experimental angular distributions cannot be obtained in these conditions, and further investigations of the excitation mechanism would be necessary.

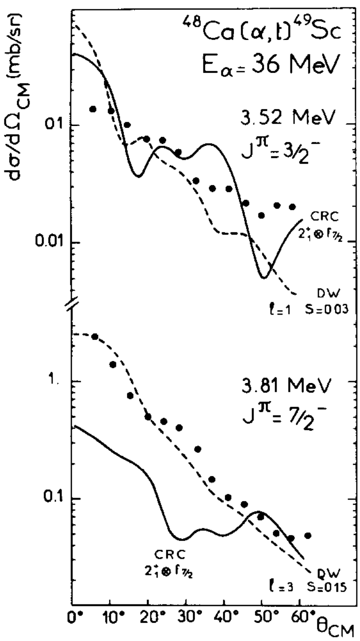

Fig. 11. Comparison or differential cross sections for one-step and two-step excitations, in the case of the $\frac{3}{2}^-$ level at 3.51 MeV and the $\frac{7}{2}^-$ level at 3.81 MeV (see text).

Finally, it may be of interest to compare the contributions of two-step processes to the total cross sections in the different proton stripping reactions. We have therefore performed some CRC calculations for two-step transitions in the (^{3}He, d) reaction at 25 MeV, in a similar way to that followed in subsect. 4.1 for (α, t), and using the optical parameters for the ^{3}He and d channels reported in paper I. Experimentally, only a few non-stripping angular distributions have been observed in the (^{3}He, d) reaction. The CRC calculations, assuming for a given level the structure proposed in subsect. 4.2, do not succeed to reproduce the data, as the two-step cross sections are found to be generally lower than the experimental ones, and the reaction mechanism is thus not completely understood in these particular cases. However, it is worth pointing out that the calculated cross sections for two-step excitation by (^{3}He, d) are generally lower by about an order of magnitude, compared with the (α, t) reaction. From this difference, it may be asserted that the results of a standard DWBA analysis should be more reliable in the case of the (^{3}He, d) reaction, compared to those obtained from (α, t).

5. Summary

We have presented in this paper a detailed study of the ^{48}Ca(α, t)^{49}Sc reaction at 36 MeV, which complements the spectroscopic information about ^{49}Sc obtained from the ^{48}Ca(^{3}He, d)^{49}Sc experiment reported in paper I. About eighty levels have been observed in the 0–7.5 MeV energy range, many of them for the first time. For a large part of these levels, the experimental angular distributions cannot be reproduced by DWBA calculations, so the eventuality for a two-step excitation has to be investigated. Non-stripping angular distributions have been compared to the results of CRC calculations, assuming weak-coupling wave functions and consequently pure two-step excitation processes. One observes a rather good agreement for a number of levels, strongly suggesting that they could be core-excited states, resulting from the coupling of one $f_{\frac{7}{2}}$ proton with low-lying excited states in ^{48}Ca. As the shapes of theoretical two-step angular distributions are characteristic of the spin and parity of the final state, J^π assignments are also proposed: in particular high spin $\frac{9}{2}^-$, $\frac{11}{2}^-$, $\frac{15}{2}^-$ and $\frac{17}{2}^+$ states are tentatively identified, based on the comparison with CRC predictions.

More generally, the CRC calculations show that two-step processes should not be neglected in the analysis of (α, t) transitions with small cross sections. As a reward for a larger complexity in the analysis, it is suggested from the present results that the (α, t) reaction could be an essential tool for the investigation of core-excited states in many other nuclei.

We wish to thank J. C. Artiges and P. Cohen for their assistance in the electronic set-up and the operating crew of the Orsay tandem for the efficient running of the accelerator. The help of Mrs Rouvet in preparing the manuscript is also acknowledged.

References

1) S. Fortier, E. Hourani, N. M. Rao and S. Galès, Nucl. Phys. **A311** (1978) 324
2) S. Fortier and S. Galès, Nucl. Phys. **A321** (1979) 137
3) A. Szanto de Toledo, H. Hafner and H. V. Klapdor, Nucl. Phys. **A320** (1979) 309; and references therein
4) P. Roussel, thèse d'État, Orsay, 1968
5) D. H. Youngblood, R. L. Kozub, R. A. Kenefick and J. C. Hiebert, Nucl. Phys. **A143** (1970) 512
6) P. Roussel, G. Bruge, A. Bussière, H. Faraggi and J. E. Testoni, Nucl. Phys **A155** (1970) 306
7) G. Bruge, H. Faraggi, Ha Duc Long and P. Roussel, rapport CEA N-1232 (1970) 124
8) P. D. Kunz, University of Colorado, report COO-535-606
9) C. M. Perey and F. G. Perey, Nucl. Data Tables **17** (1976) 1
10) O. F. Lemos, thèse de Doctorat de l'Université, Orsay (1972)
11) B. Fernandez and J. S. Blair, Phys. Rev. **C1** (1970) 523
12) F. D. Becchetti Jr. and G. W. Greenlees, in Polarization phenomena in nuclear reactions, ed. H. H. Barschall and W. Haeberli (University of Wisconsin Press, Madison, 1971) p. 682
13) P. P. Urone, L. W. Piet, H. H. Chang and B. W. Ridley, Nucl Phys. **A163** (1971) 225
14) N. S. Chant and J. N. Chang, Phys. Rev. **C14** (1976) 1763
15) N. S. Chant, Nucl. Phys. **A211** (1973) 209
16) K. W. Kemper, A. F. Zeller and T. R. Ophel, J. of Phys. **G4** (1978) L17
17) M. L. Halbert, Nucl. Data Sheets **24** (1978) 175; and references therein
18) P. D. Kunz, private communication
19) C. R. Gruhn, T. Y. Kuo, C. J. Maggiore and B. M. Preedom, Phys. Rev. **C6** (1972) 972